INFECTION AND IMMUNITY, Dec. 2001, p. 7527–7534 Vol. 69, No. 12
0019-9567/01/$04.00+0 DOI: 10.1128/IAI.69.12.7527–7534.2001

Role of RgpA, RgpB, and Kgp Proteinases in Virulence of *Porphyromonas gingivalis* W50 in a Murine Lesion Model

NEIL M. O'BRIEN-SIMPSON, RITA A. PAOLINI, BRIGITTE HOFFMANN, NADA SLAKESKI, STUART G. DASHPER, AND ERIC C. REYNOLDS*

Oral Health Sciences Unit, School of Dental Science, The University of Melbourne, Melbourne, Victoria, Australia

Received 22 November 2000/Returned for modification 27 March 2001/Accepted 11 September 2001

Extracellular Arg-x- and Lys-x-specific cysteine proteinases are considered important virulence factors and pathogenic markers for *Porphyromonas gingivalis*, a bacterium implicated as a major etiological agent of chronic periodontitis. Three genes. *rgpA*, *rgpB,* and *kgp,* encode an Arg-x-specific proteinase and adhesins (RgpA), an Arg-x-specific proteinase (RgpB), and a Lys-x-specific proteinase and adhesins (Kgp), respectively. The contribution to pathogenicity of each of the proteinase genes of *P. gingivalis* W50 was investigated in a murine lesion model using isogenic mutants lacking RgpA, RgpB, and Kgp. Whole-cell Arg-x-specific proteolytic activity of both the RgpA$^-$ and RgpB$^-$ isogenic mutants was significantly reduced (3- to 4-fold) relative to that of the wild-type W50. However, for the Kgp$^-$ isogenic mutant, whole-cell Arg-x activity was similar to that of the wild-type strain. Whole-cell Lys-x proteolytic activity of the RgpA$^-$ and RgpB$^-$ mutants was not significantly different from that of wild-type W50, whereas the Kgp$^-$ mutant was devoid of Lys-x whole-cell proteolytic activity. Sodium dodecyl sulfate-polyacrylamide gel electrophoresis and Western blot analysis using proteinase-specific antibodies of cell sonicates of the wild-type and mutant strains showed that the proteinase catalytic domain of each of the mutants was not expressed. This analysis further showed that RgpB appeared as 72- and 80-kDa bands, and the catalytic domains of RgpA and Kgp appeared as processed 45-kDa and 48-kDa bands, respectively. In the murine lesion model, mice were challenged with three doses of each mutant and wild-type strain. At the lower dose (3.0×10^9 viable-cells), no lesions were recorded for each of the mutants, whereas wild-type W50 induced large ulcerative lesions. At a dose of 6.0×10^9 viable-cells, all the mice challenged with the wild-type strain died, whereas mice challenged with the RgpA$^-$ and RgpB$^-$ isogenic mutants did not die but developed lesions. Mice challenged with the Kgp$^-$ isogenic mutant at this dose did not develop lesions. At a 1.2×10^{10} viable-cell dose, only 40% of mice challenged with the Kgp$^-$ mutant developed lesions, and these lesions were significantly smaller than lesions induced by the wild-type strain at the 3.0×10^9 viable-cell dose. All the mice challenged with the RgpA$^-$ mutant died at the 1.2×10^{10} viable-cell dose, whereas only 20% died when challenged with the RgpB$^-$ mutant at this dose. Wild-type phenotype was restored to the RgpB$^-$ mutant by complementation with plasmid pNJR12::*rgpB* containing the *rgpB* gene. There was no difference between the pNJR12::*rgpB*-complemented RgpB$^-$ mutant and the wild-type W50 strain in whole-cell Arg-x activity, protein profile, or virulence in the murine lesion model. These results show that the three proteinases, RgpA, RgpB, and Kgp, all contributed to virulence of *P. gingivalis* W50 in the murine lesion model and that the order in which they contributed was Kgp $\gg$ RgpB $\geq$ RgpA.

Porphyromonas gingivalis has been implicated as a major etiological agent in the onset and progression of chronic periodontitis, a destructive inflammatory disease of the supporting tissues of the teeth which affects between 10 and 15% of dentate adults (10, 20, 49). In a recent study, Griffen et al. (11) analyzed plaque samples from 311 subjects for the presence of heteroduplex types of *P. gingivalis*. Of the 11 different heteroduplex types detected, *P. gingivalis* W83/W50-like strains were found to be associated with periodontitis, whereas other strains, including 381-like strains, were not found to be associated with disease. This finding extends earlier animal studies in which strains W83 and W50 were classified as invasive based on their ability to cause ulcerative spreading lesions distant from the injection site, whereas strains 381 and ATCC 33277 were classified as noninvasive as they produced a localized abscess at the site of injection (29, 54). These results therefore suggest that W50 and related strains are more virulent in both animals and humans.

The pathogenicity of *P. gingivalis* has been attributed to a number of virulence factors, such as fimbriae (4), hemagglutinins (12, 13), lipopolysaccharide (LPS) (14), and the extracellular and cell-associated Arg-x- and Lys-x-specific cysteine proteinases and their associated adhesins (31, 33, 36, 45). Among these factors, the extracellular Arg-x- and Lys-x-specific cysteine proteinases are believed to play a major role in the pathogenesis of periodontal disease, as they are able to degrade a variety of host proteins and have the potential to dysregulate host defense (53).

Three genes encode the major extracellular Arg-x- and Lys-x-specific cysteine proteinases of *P. gingivalis,* and these are designated *rgpA*, *rgpB,* and *kgp* (6). We have previously characterized the proteins encoded by *rgpA* and *kgp* of strain W50 as a cell-associated complex of noncovalently associated proteinases and adhesins, designated the RgpA-Kgp proteinase-adhesin complexes, formerly the PrtR-PrtK proteinase-adhe-

* Corresponding author. Mailing address: Oral Health Sciences Unit, School of Dental Science, The University of Melbourne, 711 Elizabeth Street, Melbourne, Victoria 3000, Australia. Phone: 61 3 9341 0270. Fax: 61 3 9341 0236. E-mail: e.reynolds@unimelb.edu.au.

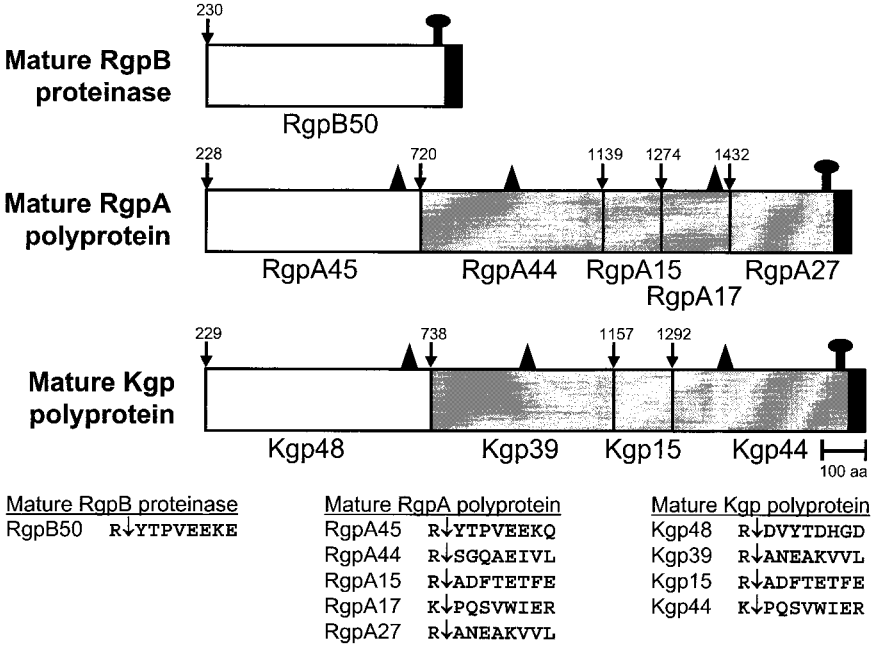

FIG. 1. Schematic representation of the processing of the RgpA and Kgp polyproteins and RgpB. The white areas indicate the catalytic domains of the proteinases, the shaded areas indicate the adhesins, and the filled C-terminal areas show the conserved C-terminal sequence proposed to be involved in secretion and cell attachment. ↑ marks the proposed outer membrane attachment to LPS. All processing sites are preceded by Arg or Lys residues (3, 46, 47). ▲ shows the location of an adhesin-binding motif proposed to be involved in binding of the RgpA45 and Kgp48 catalytic domains into large noncovalent complexes with the adhesins and in autoaggregation of the adhesins (46).

sin complexes (3). The RgpA-Kgp complexes of *P. gingivalis* strain W50 are composed of a 45-kDa Arg-x-specific proteinase (RgpA45, formerly PrtR45) associated with four sequence-related adhesins, RgpA44, RgpA15, RgpA17, and RgpA27, all encoded by *rgpA* (Fig. 1). The RgpA-Kgp complexes are also characterized by a 48-kDa Lys-x-specific proteinase (Kgp48, formerly PrtK48) associated with three sequence-related adhesins, Kgp39, Kgp15, and Kgp44, all encoded by *kgp* (3, 46, 47) (Fig. 1).

We have previously characterized the extracellular Arg-x-specific cysteine proteinase encoded by *rgpB* of strain W50 (46). This proteinase, designated RgpB, is not associated with adhesins, as the *rgpB* gene does not encode adhesins or an adhesin binding motif (Fig. 1) that is present in the RgpA and Kgp catalytic domains (46). This adhesin binding motif is also present in some of the adhesin domains of RgpA and Kgp (Fig. 1) and is proposed to be responsible for the incorporation of the RgpA and Kgp catalytic domains into noncovalently associated complexes with adhesins and for the autoaggregation of the adhesins into large complexes (46). The RgpB proteinase has been isolated as a 70- to 80-kDa membrane-associated protein and as a discrete 50-kDa protein from the culture supernatant (40, 46).

Spontaneous *P. gingivalis* mutants with reduced Arg-x and Lys-x proteinase activity and wild-type cells treated with a protease inhibitor (Nα-*p*-tosyl-L-lysine chloromethyl ketone [TLCK]) have been reported to be avirulent in animal models (16). Furthermore, a nonpigmented mutant of *P. gingivalis* W50/BE1, which has reduced Lys-x and Arg-x proteinase activity, is reported to be avirulent in animal models (26). However, this mutant also lacks gelatinase, collagenase, and dipeptidylaminopeptidase and shows reduced hemagglutinin activity, fimbrination, and extracellular vesicle production (5, 26, 43). Tokuda et al. (50, 51) have reported that two constructed isogenic mutants of *P. gingivalis* strain 381 lacking either RgpA or RgpB exhibited reduced aggregation, hemagglutination, and binding to matrix proteins relative to the wild-type 381 strain. Further, a triple mutant based on strain ATCC 33277 lacking RgpA, RgpB, and Kgp was reported not to agglutinate erythrocytes, bind to hemoglobin, or grow in defined medium containing bovine serum albumin (BSA) as the sole carbon and energy source (44). These studies suggest that the *rgpA*, *rgpB,* and *kgp* genes are important for the virulence of *P. gingivalis*.

The aim of this study therefore was to determine the virulence of isogenic mutants of the invasive W50 strain that lack the RgpA, RgpB, and Kgp proteinases in a murine lesion model.

MATERIALS AND METHODS

Bacterial strains and growth conditions. The bacteria and plasmids used in this study are listed in Table 1. Lyophilized cultures of *P. gingivalis* W50 and mutant strains (501, D7, and K1A) were grown anaerobically at 37°C on lysed horse blood agar plates supplemented with 5 μg of hemin, 0.5 μg of cysteine (HB agar) and appropriate antibiotics (1.0 μg of tetracycline and/or 10 μg of erythromycin) (<10 passages) per ml. After 3 to 4 days, colonies were used to inoculate brain heart infusion medium containing 5 μg of hemin, 0.5 μg of cysteine (25), and appropriate antibiotics (0.5 μg of tetracycline and/or 5 μg of erythromycin) per ml. Batch cultures were grown anaerobically in an MK3 Anaerobic Workstation (Don Whitley Scientific Ltd., Adelaide, Australia). Cells were harvested during exponential growth phase by centrifugation (5,000 × *g*, 30 min, 4°C) and washed twice with PG buffer (50 mM Tris-HCl, 150 mM NaCl, 5 mM $CaCl_2$, 5 mM cysteine-HCl, pH 8.0) in the anaerobic workstation for the whole-cell proteinase assays and the murine lesion model experiments. Growth

TABLE 1. Strains and plasmids

Strain or plasmid	Description	Reference
P. gingivalis		
W50	Wild type	Slakeski et al. (46)
W501	*rgpA*::*erm*	Rangarajan et al. (40)
D7	*rgpB*::*erm*	Rangarajan et al. (40)
K1A	*kgp*::*erm*	Aduse-Opoku et al. (1)
Plasmids		
pNJR12	*E. coli-Bacteroides* shuttle containing a 2.5-kb *Sst*I fragment of *tetQ*; Kan^r (*E. coli*)	Maley et al. (21)
pNJR12::*rgpB*	pNJR12 containing *rgpB*; Kan^r (*E. coli*), Tet^r (*P. gingivalis*)	This paper

of batch cultures was monitored at 650 nm using a spectrophotometer (model 295E; Perkin-Elmer). Culture purity was checked routinely by Gram stain, microscopic examination, and a variety of biochemical tests according to Slots (48).

Construction of pNJR12::*rgpB*-complemented RgpB$^-$ mutant. A PCR-derived fragment containing the *rgpB* coding region and 5′ untranslated region was generated from the λGEM-12 *P. gingivalis* genomic clone (46) using Elongase (Life Technologies) according to the manufacturer's instructions on a PC-960 thermal sequencer (Corbett Research). The PCR was performed using the forward primer (5′-GCGCGCTCTAGAGGACAGTATCTGCAACCGTCG-3′) that consists of a six base-buffer, an *Xba*I site, and bases 495 to 515 of *rgpB* (previously *prtRII;* GenBank accession no. AF007124) and the reverse primer (5′-CCGAATGGATTCCTCGGC-3′) that consists of bases 3150 to 3167 of *rgpB* in an antisense orientation. The 2.7-kb PCR product was purified using the QIAquick PCR purification kit (Qiagen Pty Ltd.) and ligated into pGEM-T Easy (Promega Corporation), transformed into *Escherichia coli* JM109 (Promega Corporation), and selected on Luria-Bertani medium (LB) containing ampicillin (100 μg/ml) following standard procedures (42).

DNA purified from transformants containing recombinant pGEM-TEasy::*rgpB* was digested with *Xba*I and *Sal*I (Promega Corporation), and the insert was purified and ligated into the *E. coli-Bacteroides* shuttle vector pNJR12 that had been digested with *Xba*I and *Sal*I. The construct was used to transform *E. coli* JM109, which was then plated on LB agar containing kanamycin (50 μg/ml). The *rgpB* insert in the purified pNJR12::*rgpB* construct was verified by DNA sequencing. The verified construct was then used to transform electrocompetent *P. gingivalis* W50D7. The procedure for transformation and preparation of cells was essentially that of Fletcher et al. (9) except that transformed cells were grown to an optical density at 650 nm (OD_{650}) of 0.5 and selected on HB agar containing 10 μg of erythromycin and 1 μg of tetracycline per ml after 7 to 10 days of incubation at 37°C under anaerobic conditions.

Arg-x-specific and Lys-x-specific whole-cell proteinase assays. *P. gingivalis* cells (W50 and mutants 501, D7, and K1A) were harvested under anaerobic conditions at early exponential, mid-late exponential, and stationary growth phases (0.5, 0.9, and 1.25 $O.D._{650}$, respectively) by centrifugation (5,000 × *g*, 30 min, 4°C), washed, and resuspended in PG buffer (1 ml). Resuspended cells were analyzed immediately for Arg-x and Lys-x proteolytic activity using *N*-α-benzoyl-L-Arg-*p*-nitroanilide (Bz-Arg-pNA; Sigma) and benzyloxycarbonyl-L-Lys-*p*-nitroanilide (Bz-Lys-pNA; Sigma). These enzyme substrates were prepared as follows: 2 mM Bz-Arg-pNA or 2 mM Bz-Lys-pNA in 3 ml of isopropyl alcohol was subjected to sonication for 10 min, after which 7 ml of enzyme buffer (400 mM Tris-HCl, 100 mM NaCl, 20 mM cysteine, pH 8.0) was added. Amidolytic activity is expressed as units (micromoles of substrate converted per minute) at 37°C.

Resuspended cells (16 or 32 μl) were diluted in PG buffer (total volume, 360 μl), and 40 μl of fresh 100 mM cysteine-HCl (pH 8.0) was added. After incubation for 10 min at 37°C, 400 μl of Arg or Lys substrate buffer was added, and proteinase activity was measured every 10 s for 3 min at 37°C using a Hewlett Packard 8452A diode array spectrophotometer (Hewlett Packard, Melbourne, Australia) at a wavelength of 410 nm. Proteolytic activity data were statistically analyzed using a one-way classification analysis of variance with a post hoc Scheffe test.

SDS-PAGE and Western blot analysis of *P. gingivalis* W50 and mutant cell sonicates. *P. gingivalis* strain W50 wild-type, mutants, and pNJR12::*rgpB*-complemented RgpB$^-$ mutant were grown in batch culture and harvested at late exponential phase by centrifugation (5,000 × *g*, 20 min, 4°C). Cells were washed once with 50 ml of TC buffer (20 mM Tris-HCl, 5 mM $CaC1_2$) containing 150 mM NaCl, pH 7.4, and sonicated at 4°C as previously described (3). The harvesting of cells and sonication were also performed with 10 mM TLCK in the buffer, with fresh 10 mM TLCK being added at every step. The sonicates were recentrifuged at 4°C for 10 min, and the collected supernatants were stored at −70°C. The protein concentration of each cell sonicate was determined by using the Bradford protein assay (Bio-Rad, North Ryde, New South Wales, Australia) with BSA as the standard. Each cell sonicate (10 μg of protein) was subjected to sodium dodecyl sulfate-polyacrylamide gel electrophoresis (SDS-PAGE) in gels of 12.5% (wt/vol) acrylamide (1 mm) by the method of Laemmli (18) with a minigel system (Bio-Rad, North Ryde, New South Wales, Australia). Proteins were electrophoretically transferred onto a polyvinylidene difluoride (PVDF) membrane as described previously (8). After sectioning of the membrane, one section was stained with 0.1% (wt/vol) CBB R250, and the remaining section was blocked for 1 h at 20°C with 5% (wt/vol) nonfat skim milk powder in TN buffer (50 mM Tris-HCl [pH 7.4], 100 mM NaCl) and incubated with proteinase-specific antibody (32) diluted 1:25 with TN buffer.

The proteinase-specific antibody was raised in mice using a synthetic peptide conjugated to diphtheria toxoid (32). The synthetic peptide contained the putative active-site His and flanking amino acid sequence (HGSETAW) of RgpA/B and Kgp. After 5 h at 20°C, the section was washed with 4× TN buffer containing 0.05% (vol/vol) Tween 20 and then incubated for 1 h at 20°C with anti-mouse immunoglobulin G-horseradish peroxidase conjugate (Sigma-Aldrich, Sydney, New South Wales, Australia). After washing with 4× TN buffer containing 0.05% (vol/vol) Tween 20, bound antibody was detected with 0.05% (wt/vol) 4-chloro-1-naphthol in TN buffer containing 16.6% (vol/vol) methanol and 0.015% (vol/vol) H_2O_2. Color development was stopped by rinsing the membranes with water.

Murine lesion model. The murine lesion model experiments were approved by the University of Melbourne Ethics Committee for Animal Experimentation and were conducted essentially as described previously (32). BALB/c mice 6 to 8 weeks old (10 animals per group) were challenged with either 3.0×10^9, 6.0×10^9, or 1.2×10^{10} viable cells of *P. gingivalis* strain W50 and mutants 501, D7, and K1A by subcutaneous injection (100 μl) in the abdomen, and lesion size and mortality were monitored over 14 days as described previously (32). Mice were also challenged with 3.0×10^9 and 6.0×10^9 viable cells of the RgpB$^-$ mutant D7 carrying the pNJR12 vector and the pNJR12::*rgpB*-complemented RgpB$^-$ mutant. The *P. gingivalis* inocula were prepared using PG buffer in the anaerobic workstation as described above. The number of viable cells in each inoculum was verified by enumeration on HB agar. The maximum sizes of the lesions developed were statistically analyzed using the Kruskal-Wallis test and Mann-Whitney *U*-Wilcoxon rank sum test with a Bonferroni correction for type 1 error (30).

RESULTS

Arg-x and Lys-x whole-cell proteinase activity of RgpA$^-$, RgpB$^-$, and Kgp$^-$ mutants of *P. gingivalis* W50. Whole-cell Arg-x and Lys-x proteinase activity was measured at the early exponential, mid-late exponential, and early stationary phases of growth for each of the isogenic mutants and wild-type strain (Fig. 2 and 3). The whole-cell Arg-x activity (in units per 10^{11} cells) (Fig. 2) of the Kgp$^-$ strain was found not to be significantly different at each growth phase measured compared with the wild-type strain. For both the Kgp$^-$ mutant and wild-type strain, the Arg-x activity at the early exponential phase of growth was significantly ($P < 0.05$) less (28%) than that at later growth phases. There was a significant ($P < 0.001$) difference in the Arg-x activity of both the RgpA$^-$ and RgpB$^-$ mutants compared with the wild-type strain. The Arg-x-specific whole-cell activity of both these mutants was consistently lower (3- to

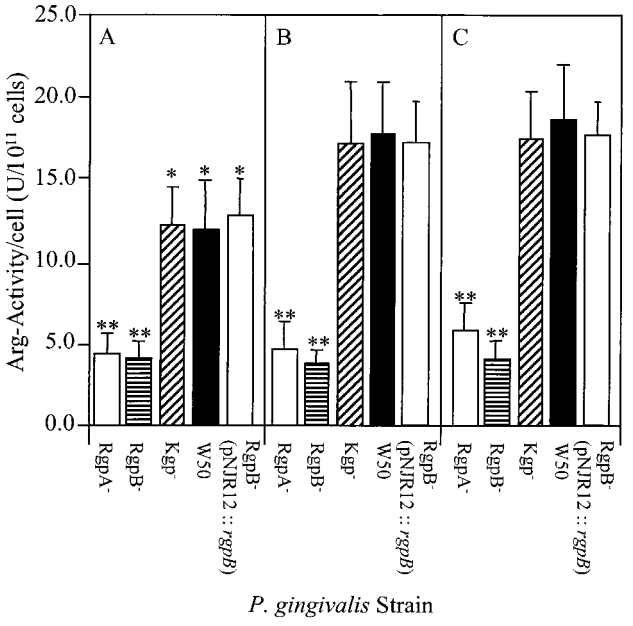

FIG. 2. Whole-cell Arg-x proteolytic activity of *P. gingivalis* W50 and RgpA$^-$, RgpB$^-$, and Kgp$^-$ isogenic mutants and pNJR12::*rgpB*-complemented RgpB$^-$ mutant at different phases of growth. *P. gingivalis* cells were harvested anaerobically at early (A) and late (B) exponential and stationary (C) growth phases. Harvested cells were centrifuged, resuspended in PG buffer, and assayed for Arg-x proteolytic activity. Data presented represent the mean ± standard deviation (SD) of three separate experiments. *, groups significantly different ($P < 0.05$) from activity at later phases of growth. **, groups significantly different ($P < 0.001$) from activity of *P. gingivalis* wild-type W50 strain.

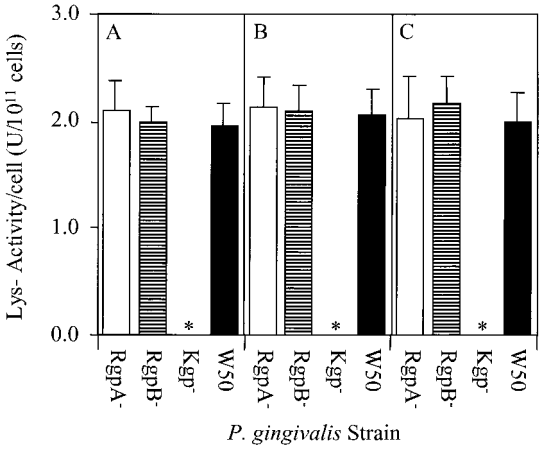

FIG. 3. Whole-cell Lys-x proteolytic activity of *P. gingivalis* W50 and RgpA$^-$, RgpB$^-$ and Kgp$^-$ isogenic mutants at different phases of growth. *P. gingivalis* cells were harvested anaerobically at early (A) and late (B) exponential and stationary (C) growth phases. Harvested cells were centrifuged, resuspended in PG buffer, and assayed for Lys-x proteolytic activity. Data presented represent the mean ± SD of three separate experiments. *, no whole-cell Lys-x proteolytic activity was detected for the Kgp$^-$ mutant.

4-fold) than that of the wild-type strain at each growth phase measured. However, the Arg-x activities of the RgpA$^-$ and RgpB$^-$ mutants were not significantly different from each other and did not increase with growth.

Whole-cell Lys-x activity of RgpA$^-$and RgpB$^-$ mutants and the wild type did not increase with growth as seen with the wild-type Arg-x activity, and there was no significant difference between strains (Fig. 3). No whole-cell Lys-x proteolytic activity was detected for the Kgp$^-$ mutant at any stage of growth.

SDS-PAGE and Western blot analysis of RgpA$^-$, RgpB$^-$, and Kgp$^-$ mutants of *P. gingivalis* W50. Cell sonicates of *P. gingivalis* W50 and RgpA$^-$, RgpB$^-$, and Kgp$^-$ mutants were subjected to SDS-PAGE and Western blot analysis using the proteinase-specific antibody (Fig. 4). The Western blot of the wild-type W50 sonicate prepared in the absence of TLCK (Fig. 4A) revealed diffuse immunoreactive bands at 45 kDa, 48 kDa, and 70 to 90 kDa. The same analysis of the proteinase isogenic mutants showed that the 48-kDa band in Kgp$^-$, the 45-kDa band in RgpA$^-$ and the 70- to 90-kDa diffuse band in RgpB$^-$ were not detected, confirming the genotype of the three mutants and the previous assignment of these bands (3, 40). However, when the cell sonicates were prepared in the presence of 10 mM TLCK, the bands obtained on the Western blot were less diffuse, suggesting that TLCK was inhibiting proteolytic processing during preparation of the sample (Fig. 4B).

The Western blot of the wild-type W50 in the presence of 10 mM TLCK also showed the 45-kDa RgpA45 and 48-kDa Kgp48 processed catalytic domains. However, in the presence of TLCK, the diffuse 70- to 90-kDa band resolved into two major bands at 72 and 80 kDa. Western blot analysis of the isogenic mutants in the presence of 10 mM TLCK confirmed that the 45-kDa band was RgpA45 and that the 48-kDa band was Kgp48, although interestingly, the 48-kDa band resolved into two bands in the RgpA$^-$ and RgpB$^-$ mutants, suggesting a role for these Arg-x-specific proteinases in the processing of Kgp. Similarly, RgpA45 appeared at a slightly higher molecu-

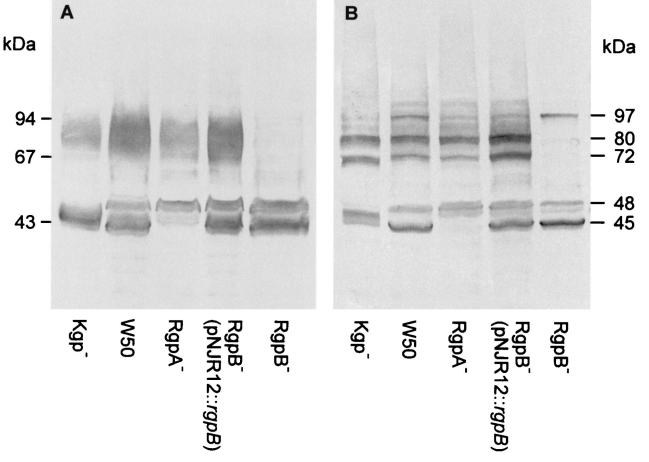

FIG. 4. Western blot analysis of cell sonicates of isogenic mutants RgpA$^-$, RgpB$^-$, and Kgp$^-$, pNJR12::*rgpB*-complemented RgpB$^-$ mutant, and wild-type strain using proteinase-specific sera. (A) Cell sonicate. (B) Cell sonicate prepared in the presence of 10 mM TLCK. The cell sonicates were subjected to SDS-PAGE and transferred onto a PVDF membrane. The membranes were probed with sera (1:25 in TN buffer) from mice immunized with a synthetic peptide which has the sequence HGSETAW that is common to each proteinase (32). Positions of molecular mass markers are indicated (in kilodaltons).

lar weight in the Kgp$^-$ mutant, perhaps suggesting a role for the Lys-x-specific enzyme in processing of RgpA.

The Western blot of the RgpB$^-$ mutant in the presence of TLCK suggested that all the bands that appeared between 70 and 90 kDa, including the two major bands at 72 kDa and 80 kDa, were isoforms of RgpB. Interestingly, a band at 97 kDa was present in the Western blot of the wild-type W50 and RgpB$^-$ and RgpA$^-$ mutants in the presence of 10 mM TLCK which may be a partially processed form of Kgp. The Western blot analysis therefore confirmed the genotypes and the proteolytic enzyme profiles of the three isogenic mutants and suggested a role for each proteinase in the processing of the others. Western blot analysis of outer membranes of the wild-type W50 and isogenic mutants prepared in the presence and absence of 10 mM TLCK produced the same results as the cell sonicates shown in Fig. 4 (data not shown).

Characterization of pNJR12::*rgpB*-complemented RgpB$^-$ mutant. A cell sonicate of the pNJR12::*rgpB*-complemented RgpB$^-$ mutant was subjected to SDS-PAGE and Western blot analysis using the proteinase-specific antibodies (Fig. 4). This analysis showed that the pNJR12::*rgpB*-complemented mutant had immunoreactive bands corresponding to the RgpA (45 kDa) and Kgp (48 kDa) catalytic domains as well as the 72- and 80-kDa immunoreactive protein bands corresponding to the RgpB proteinase. The intensity of the 72- and 80-kDa immunoreactive bands was similar to the same immunoreactive bands for the wild-type W50 strain. The bands, however, were absent in the Western blot of the RgpB$^-$ mutant D7 (Fig. 4).

Whole-cell Lys-x proteolytic activity of the pNJR12::*rgpB*-complemented mutant was not affected by the transformation, as there was no significant difference in the Lys-x activity compared with the wild-type W50 or the RgpB$^-$ mutant D7 at each growth phase measured (data not shown). The whole-cell Arg-x proteolytic activity of the pNJR12::*rgpB*-complemented mutant was found to be restored to a similar level to that of the wild-type W50 strain (Fig. 2), which was 3- to 4-fold higher than that of the RgpB$^-$ mutant D7 at each growth phase measured. There was also a significantly ($P < 0.05$) lower whole-cell Arg-x activity for the pNJR12::*rgpB*-complemented mutant in the early exponential growth phase compared with the same activity at later growth phases, as shown for the wild-type strain (Fig. 2).

Virulence of RgpA$^-$, RgpB$^-$, Kgp$^-$, and pNJR12::*rgpB*-complemented RgpB$^-$ mutants in the murine lesion model. To evaluate the virulence of the isogenic mutants, BALB/c mice were challenged subcutaneously with the RgpA$^-$, RgpB$^-$ and Kgp$^-$ mutants as well as the wild-type W50 strain at three doses, 3.0×10^9, 6.0×10^9 and 1.2×10^{10} viable cells. Lesions that developed were measured, and the maximum lesion size for each strain is shown in Fig. 5 A, B, and C. At the 3.0×10^9 viable-cell dose, only mice challenged with the wild-type W50 strain developed lesions. All the mice challenged with the wild-type W50 strain at the 6.0×10^9 viable-cell dose died 3 days after the inoculation. Both the RgpA$^-$ and RgpB$^-$ mutants induced lesions in all of the mice at the 6.0×10^9 viable-cell dose, and the lesion sizes were not significantly different from those induced by the wild-type W50 strain at the 3.0×10^9 viable-cell dose. However, no lesions were recorded for mice challenged with the Kgp$^-$ mutant at the 6.0×10^9 viable-cell dose. The 1.2×10^{10} viable-cell dose induced 100% mortality in mice inoculated with the RgpA$^-$ mutant and wild-type W50 strain. Challenge with the RgpB$^-$ mutant at the 1.2×10^{10} viable-cell dose resulted in only 20% mortality and an average increase of 35% in the lesion size compared with the lesions induced by the same mutant at the 6.0×10^9 viable-cell dose. In contrast, none of the mice challenged with the Kgp$^-$ mutant at the 1.2×10^{10} viable-cell dose died, and only 40% of the animals developed lesions. The mean lesion size produced by the Kgp$^-$ mutant at this dose was significantly ($P < 0.001$) smaller than that induced by the RgpB$^-$ mutant at the same dose and by the wild-type W50 strain at the 3.0×10^9 viable-cell dose.

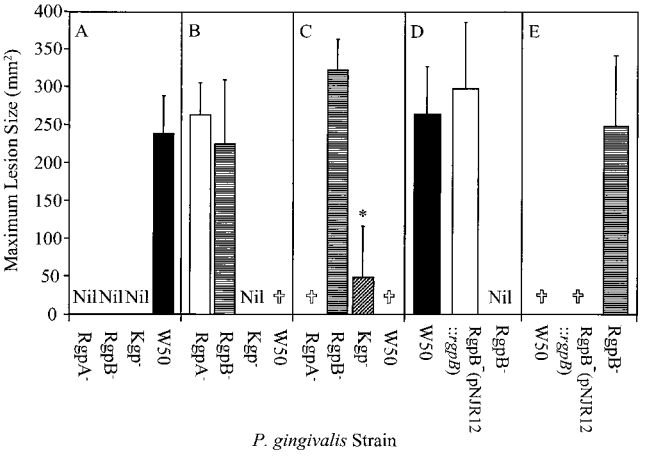

FIG. 5. Maximum lesion size of mice challenged with *P. gingivalis* W50, RgpA$^-$, RgpB$^-$, and Kgp$^-$ isogenic mutants, and pNJR12::*rgpB*-complemented RgpB$^-$ mutant. BALB/c mice were challenged subcutaneously with 3.0×10^9 (A), 6.0×10^9 (B), or 1.2×10^{10} (C) viable *P. gingivalis* W50 and isogenic mutant cells and with 3.0×10^9 (D) and 6.0×10^9 (E) viable *P. gingivalis* W50, RgpB$^-$ isogenic mutant, and pNJR12::*rgpB*-complemented RgpB$^-$ mutant cells. Animals were monitored over a 14-day period for mortality and lesion size. Data presented in panels A to E represent mean ± SD ($n = 10$) from separate experiments and were analyzed using the nonparametric Mann-Whitney *U*-Wilcoxon rank sum test. *, group significantly different ($P < 0.001$) from RgpB$^-$ at same dose and from wild-type W50 strain at the 3.0×10^9 viable-cell dose. †, 100% mortality. Nil, no lesions observed.

Mice were also challenged with 3.0×10^9 and 6.0×10^9 viable cells of the RgpB$^-$ mutant D7 carrying the pNJR12 vector, the pNJR12::*rgpB*-complemented RgpB$^-$ mutant, and the wild-type W50 strain (Fig. 5D and E). At the 3.0×10^9 viable-cell dose, the pNJR12::*rgpB*-complemented RgpB$^-$ mutant induced lesions in all of the mice, and the mean lesion size was not significantly different from that induced by the wild-type W50 strain at the same dose. Inoculation of mice with the pNJR12::*rgpB*-complemented RgpB$^-$ mutant at the 6.0×10^9 viable-cell dose induced 100% mortality within 3 days, which was consistent with the level of mortality induced by the wild-type W50 strain at the same dose. Challenge with the RgpB$^-$ mutant carrying the pNJR12 vector without the *rgpB* insert did not result in lesions at the 3.0×10^9 viable-cell dose and did not result in mortality at the 6.0×10^9 viable-cell dose.

DISCUSSION

In this study, the role of the Arg-x (RgpA and RgpB) and Lys-x (Kgp) proteinases in virulence of *P. gingivalis* was investigated in the murine lesion model using three isogenic mutants lacking the proteinases. Subjecting each of the isogenic mutants to SDS-PAGE and Western blot analysis with a proteinase-specific antibody showed that each of these proteinases was absent in the Western blot. The analysis of the form of the RgpA, RgpB, and Kgp proteinases of the wild type and the three isogenic mutants by SDS-PAGE and Western blot revealed that RgpB appeared as 72- and 80-kDa bands and the majority of RgpA and Kgp appeared as fully processed 45-kDa and 48-kDa catalytic domains, respectively. These results therefore are consistent with the previous characterization of these cell surface proteins (3, 46).

It has been proposed previously (3, 46) that the RgpA and Kgp polyproteins are secreted and then attached to the outer membrane, possibly through the conserved C-terminal segment (Fig. 1), as this segment is not found in the soluble RgpA-Kgp complexes released from the outer membrane (3, 36; unpublished data). As the N-terminal residue of the activated catalytic domains of RgpA, Kgp, and RgpB is a residue C-terminal to an Arg (3, 46), it is likely that the polyproteins are processed (activated) at these Arg residues to remove their profragments to produce mature 160-kDa (RgpA) and 163-kDa (Kgp) forms (Fig. 1). These mature RgpA and Kgp polyproteins must then undergo further processing at Arg and Lys residues (probably autolytic) to release the proteinase catalytic domains and several C-terminal sequence-related adhesin domains (Fig. 1) that have been characterized previously (3, 36, 47).

We have shown (46) that both the RgpA and Kgp catalytic domains, but not RgpB, contain a C-terminal adhesin-binding motif that is also found in the released adhesins (Fig. 1). Through this adhesin-binding motif, the proteinase catalytic domains may bind to their respective adhesins, which in turn may aggregate and bind to the putative anchored C-terminal adhesin, localizing RgpA and Kgp as noncovalently associated processed domains on the cell surface. The 50-kDa mature RgpB is presumably attached directly to the cell surface to form the membrane-associated 72- and 80-kDa forms (Fig. 1). This is supported by the work of Curtis et al. (7), who have shown that the 70- to 80-kDa membrane-associated form of RgpB, but not the 50-kDa isoform found in the culture supernatant, is immunoreactive with anti-LPS antibodies. In the presence of 10 mM TLCK, RgpB appeared as two major bands at 72 kDa and 80 kDa in the current study, which presumably represent two differently LPS-modified isoforms of the enzyme. The proposed C-terminal attachment of RgpB is also consistent with the work of Potempa et al. (39), who have shown that the 50-kDa isoform in the culture supernatant is C-terminally truncated by processing before the putative anchor sequence.

The processing of RgpA and Kgp, once secreted, to release the proteinase catalytic domains and the adhesin domains is thought to be autolytic, as the processing sites always involve Arg or Lys residues (Fig. 1). The slight change in molecular weight of the processed domains obtained in the Western blots of each of the isogenic mutants (Fig. 4) is consistent with a processing role for these enzymes. Furthermore, the 3- to 4-fold reduction in cell surface Arg-x-specific proteolytic activity upon inactivation of either *rgpA* or *rgpB* is also consistent with a processing role for both of these enzymes. It is interesting, however, that inactivating any one of the three proteinase genes did not abolish secretion and processing of the other two gene products. As multiple Arg and Lys residues exist between the processed domains of the polyproteins, it is very likely that any one of the proteinases can facilitate processing of the others.

The whole-cell Arg-x-specific proteolytic activity of both the Kgp^- mutant and W50 wild-type strain was significantly less at the early exponential phase of growth and increased to a plateau at the mid-exponential phase. This increase in activity was not observed for the Lys-x activity of the $RgpA^-$ and $RgpB^-$ mutants or the wild-type W50 strain. In fact, the Lys-x-specific proteolytic activity of the wild-type and $RgpA^-$ and $RgpB^-$ mutants was similar at all phases of growth. The unchanged Lys-x proteolytic activity for the $RgpA^-$ and $RgpB^-$ mutants is in contrast to the findings of Tokuda et al. (52), who have reported that inactivation of the $RgpA^-$ gene in strain 381 resulted in downregulation of the *kgp* gene, as indicated by Northern blot analysis. However, whole-cell Arg-x and Lys-x proteolytic activities were not measured in that study. The data reported here suggest that Arg-x activity but not Lys-x activity may be influenced by growth phase or environmental factors. This is consistent with several earlier reports that have shown that environmental factors, such as hemin availability, pH, and temperature, can affect the Arg-x-specific proteolytic activity of *P. gingivalis* (22, 24, 35).

Inactivation of the *rgpA*, *rgpB,* and *kgp* genes, as well as reducing whole-cell proteolytic activity, also resulted in a measurable reduction in the pathogenicity of each mutant in the murine lesion model. No lesions were recorded for mice challenged with the 3.0×10^9 viable-cell dose for any of the mutants, but increasing the challenge dose resulted in differences in virulence for each of the isogenic mutants. Interestingly, although the Arg-x activity of the $RgpA^-$ and $RgpB^-$ mutants was similar, there was a significant difference in virulence at the 1.2×10^{10} viable-cell dose, with 100% mortality of mice challenged with the $RgpA^-$ mutant. The $RgpB^-$ mutant, however, at the same dose induced only 20% mortality.

The *rgpA* gene in W50 produces a noncovalently associated proteinase-adhesin complex (3). The *rgpB* gene in W50 produces two isoforms of RgpB that are not associated with adhesins, 72- and 80-kDa membrane-attached forms (40;this study) and a 50-kDa discrete proteinase in the culture supernatant (40, 46). The adhesins of the RgpA proteinase-adhesin complex have been shown to bind to host substrates, facilitating proteolysis (37). This targeting role of the adhesins has been speculated to increase the virulence of the proteinase. However, the results of this study suggest that RgpB may have a greater role in virulence. Recently, Tokuda et al. (50, 51) constructed $RgpA^-$ and $RgpB^-$ isogenic mutants of strain 381 and reported marked changes in surface and binding properties of the two mutants relative to the wild type. The authors noted differences between the two mutants, with the $RgpB^-$ mutant exhibiting a reduced ability to bind to epithelial cells. These and other studies (15, 28), showing pleiotropic effects of inactivation of the *rgpA* and *rgpB* genes, suggest that the Arg-

x-specific proteolytic activity of *P. gingivalis* is involved in processing of not only the proteinases but also other surface proteins. Therefore, a greater role in pathogenicity for RgpB may reflect a greater role in processing for this enzyme.

The least virulent of the isogenic mutants in the murine lesion model was the Kgp$^-$ mutant, as only 40% of mice challenged with the 1.2×10^{10} viable-cell dose developed lesions and these were significantly smaller than the lesions induced by the wild-type strain at the 3.0×10^9 viable-cell dose. Kgp has been reported to be involved in hemoglobin binding and degradation and heme accumulation (17, 19, 34, 38). The nonpigmented phenotype of the Kgp$^-$ mutant (K1A) is consistent with the proposed role of this proteinase in heme accumulation. Heme has been reported to be essential for the growth and virulence of *P. gingivalis* (23), and thus the Kgp$^-$ mutant's reduced ability to accumulate heme may account for its reduced virulence in the murine lesion model.

In this study we also investigated the complementation of the RgpB$^-$ mutant with a plasmid containing the *rgpB* gene. Whole-cell Arg-x-specific proteolytic activity was fully restored by the complementation. The pNJR12::*rgpB*-complemented RgpB$^-$ mutant also displayed the same pattern of Arg-x activity/cell as the wild-type strain, with a lower activity at early exponential growth phase which increased in later phases of growth. Although pNJR12 is a low-copy-number plasmid, it may have been expected that the pNJR12::*rgpB*-complemented RgpB$^-$ mutant would have exhibited higher Arg-x activity than the wild-type W50 strain due to the presence of multiple copies of the plasmid and therefore of the *rgpB* gene. As an increase in Arg-x-specific activity was not observed, this suggests that the expression of the *rgpB* gene is regulated, which is again consistent with earlier reports of Arg-x proteolytic activity regulation (22, 24, 35).

The characteristic 72- and 80-kDa RgpB bands were also observed for the complemented RgpB$^-$ mutant, indicating that the plasmid-expressed RgpB was secreted and attached to the outer membrane in the same manner as the protein in the wild-type W50 strain. As well as restoring the enzymatic and protein profile, the pNJR12::*rgpB* complementation fully restored pathogenicity in the murine lesion model. Using techniques similar to those described here for mutant complementation, others have shown the importance of specific genes and their products for the virulence of *Listeria monocytogenes*, *Proteus mirabilis*, *Vibrio anguillarum*, and *Yersinia enterocolitica* (2, 27, 41, 55).

In conclusion, by characterizing the virulence of *P. gingivalis* isogenic mutants 501, D7, and K1A, lacking RgpA, RgpB, and Kgp, respectively, and the pNJR12::*rgpB*-complemented RgpB$^-$ mutant in the murine lesion model, we have shown that the three proteinases all contributed to virulence in this model and that the order of contribution was Kgp $\gg$ RgpB $\geq$ RgpA.

ACKNOWLEDGMENTS

We are grateful to Michael Curtis and Joseph Aduse-Opoku for supplying the *P. gingivalis* mutants 501, D7, and K1A.

This work was supported by the Australian National Health and Medical Research Council (Project No. 990199).

REFERENCES

1. **Aduse-Opoku, J., N. N. Davies, A. Gallagher, A. Hashim, H. E. Evans, M. Rangarajan, J. M. Slaney, and M. A. Curtis.** 2000. Generation of Lys-gingipain protease activity in *Porphyromonas gingivalis* W50 is independent of Arg-gingipain protease activities. Microbiology **146:**1933–1940.
2. **Bahrani, F. K., G. Massad, C. V. Lockatell, D. E. Johnson, R. G. Russell, J. W. Warren, and H. L. Mobley.** 1994. Construction of an MR/P fimbrial mutant of *Proteus mirabilis*: role in virulence in a mouse model of ascending urinary tract infection. Infect. Immun. **62:**3363–3371.
3. **Bhogal, P. S., N. Slakeski, and E. C. Reynolds.** 1997. A cell-associated protein complex of *Porphyromonas gingivalis* W50 composed of Arg- and Lys-specific cysteine proteinases and adhesins. Microbiology **143:**2485–2495.
4. **Chandad, F., and C. Mouton.** 1995. Antigenic, structural, and functional relationships between fimbriae and the hemagglutinating adhesin HA-Ag2 of *Porphyromonas gingivalis*. Infect. Immun. **63:**4755–4763.
5. **Collinson, L. M., M. Rangarajan, and M. A. Curtis.** 1998. Altered expression and modification of proteases from an avirulent mutant of *Porphyromonas gingivalis* W50 (W50/BE1). Microbiology **144:**2487–2496.
6. **Curtis, M. A., H. K. Kuramitsu, M. Lantz, F. L. Macrina, K. Nakayama, J. Potempa, E. C. Reynolds, and J. Aduse-Opoku.** 1999. Molecular genetics and nomenclature of proteases of *Porphyromonas gingivalis*. J. Periodont. Res. **34:**464–472.
7. **Curtis, M. A., A. Thickett, J. M. Slaney, M. Rangarajan, J. Aduse-Opoku, P. Shepherd, N. Paramonov, and E. F. Hounsell.** 1999. Variable carbohydrate modifications to the catalytic chains of the RgpA and RgpB proteases of *Porphyromonas gingivalis* W50. Infect. Immun. **67:**3816–3823.
8. **Dashper, S. G., N. M. O'Brien-Simpson, P. S. Bhogal, A. D. Franzmann, and E. C. Reynolds.** 1998. Purification and characterization of a putative fimbrial protein/receptor of *Porphyromonas gingivalis*. Aust. Dent. J. **43:**99–104.
9. **Fletcher, H. M., H. A. Schenkein, R. M. Morgan, K. A. Bailey, C. R. Berry, and F. L. Macrina.** 1995. Virulence of a *Porphyromonas gingivalis* W83 mutant defective in the *prtH* gene. Infect. Immun. **63:**1521–1528.
10. **Fox, C. H.** 1992. New considerations in the prevalence of periodontal disease. Curr. Opin. Dent. **2:**5–11.
11. **Griffen, A. L., M. R. Becker, S. R. Lyons, M. L. Moeschberger, and E. J. Leys.** 1999. Prevalence of *Porphyromonas gingivalis* and periodontal health status. J. Clin. Microbiol. **36:**3239–3242.
12. **Han, N., J. Whitlock, and A. Progulske Fox.** 1996. The hemagglutinin gene A (*hagA*) of *Porphyromonas gingivalis* 381 contains four large, contiguous, direct repeats. Infect. Immun. **64:**4000–4007.
13. **Hinode, D., K. Masuda, M. Yoshioka, K. Watanabe, T. Umemoto, D. Grenier, D. Mayrand, and R. Nakamura.** 1995. Immunological characterization and localization of a *Porphyromonas gingivalis* BApNA-hydrolyzing protease possessing hemagglutinating activity. FEMS Microbiol. Lett. **131:**211–217.
14. **Holt, S. C., and T. E. Bramanti.** 1991. Factors in virulence expression and their role in periodontal disease pathogenicity. Crit. Rev. Oral Biol. Med. **2:**177–281.
15. **Kadowaki, T., K. Nakayama, F. Yoshimura, K. Okamoto, N. Abe, and K. Yamamoto.** 1998. Arg-gingipain acts as a major processing enzyme for various cell surface proteins in *Porphyromonas gingivalis*. J. Biol. Chem. **273:** 29072–29076.
16. **Kesavalu, L., S. C. Holt, and J. L. Ebersole.** 1997. *Porphyromonas gingivalis* virulence in a murine lesion model: effects of immune alterations. Microb. Pathog. **23:**317–326.
17. **Kuboniwa, M., A. Amano, and S. Shizukuishi.** 1998. Hemoglobin-binding protein purified from *Porphyromonas gingivalis* is identical to lysine-specific cysteine proteinase (Lys-gingipain). Biochem. Biophys. Res. Commun. **249:** 38–43.
18. **Laemmli, U. K.** 1970. Cleavage of structural proteins during the assembly of the head of bacteriophage T4. Nature **227:**680–685.
19. **Lewis, J. P., J. A. Dawson, J. C. Hannis, D. Muddiman, and F. L. Macrina.** 1999. Hemoglobinase activity of the lysine gingipain protease (Kgp) of *Porphyromonas gingivalis* W83. J. Bacteriol. **181:**4905–4913.
20. **Maiden, M. F. J., R. J. Carman, M. A. Curtis, I. R. Gillett, G. S. Griffiths, J. A. C. Sterne, W. J. M. A., and N. W. Johnson.** 1990. Detection of high-risk groups and individuals for periodontal diseases: laboratory markers based on the microbiological analysis of subgingival plaque. J. Clin. Periodontol. **17:** 1–13.
21. **Maley, J., N. B. Shoemaker, and I. S. Roberts.** 1992. The introduction of colonic-*Bacteroides* shuttle plasmids into *Porphyromonas gingivalis*: identification of a putative *P. gingivalis* insertion-sequence element. FEMS Microbiol. Lett. **72:**75–81.
22. **Marsh, P. D., A. S. McKee, and A. S. McDermid.** 1988. Effect of haemin on enzyme activity and cytotoxin production by *Bacteroides gingivalis* W50. FEMS Microbiol. Lett. **55:**87–92.
23. **Marsh, P. D., A. S. McDermid, A. S. McKee, and A. Baskerville.** 1994. The effect of growth rate and haemin on the virulence and proteolytic activity of *Porphyromonas gingivalis* W50. Microbiology **140:**861–865.
24. **McDermid, A. S., A. S. McKee, and P. D. Marsh.** 1988. Effect of environmental pH on enzyme activity and growth of *Bacteroides gingivalis* W50. Infect. Immun. **56:**1096–1100.
25. **McKee, A. S., A. S. McDermid, A. Baskerville, A. B. Dowsett, D. C. Ellwood, and P. D. Marsh.** 1986. Effect of hemin on the physiology and virulence of *Bacteroides gingivalis* W50. Infect. Immun. **52:**349–355.
26. **McKee, A. S., A. S. McDermid, R. Wait, and A. Baskerville.** 1988. Isolation

of colonial variants of *Bacteroides gingivalis* W50 with reduced virulence. J. Med. Microbiol. **27:**59–64.
27. **Milton, D. L., O. T. R., P. Horstedt, and H. Wolf-Watz.** 1996. Flagellin A is essential for the virulence of *Vibrio anguillarum*. J. Bacteriol. **178:**1310–1319.
28. **Nakayama, K., F. Yoshimura, T. Kadowaki, and K. Yamamoto.** 1996. Involvement of arginine-specific cysteine proteinase (Arg-gingipain) in fimbriation of *Porphyromonas gingivalis*. J. Bacteriol. **178:**2818–2824.
29. **Neiders, M. E., P. B. Chen, H. Suido, H. S. Reynolds, J. J. Zambon, M. Shlossman, and R. J. Genco.** 1989. Heterogeneity of virulence of *Bacteroides gingivalis*. J. Periodont. Res. **24:**192–198.
30. **Norusis, M.** 1993. SPSS for Windows: base system user's guide, release 6.0. SPSS Inc., Chicago, Ill.
31. **O'Brien-Simpson, N. M., C. L. Black, P. S. Bhogal, S. M. Cleal, N. Slakeski, T. J. Higgins, and E. C. Reynolds.** 2000. Serum IgG and IgG subclass responses to the RgpA-Kgp proteinase-adhesin complex of *P. gingivalis* in adult periodontitis. Infect. Immun. **68:**2704–2712.
32. **O'Brien-Simpson, N. M., R. Paolini, and E. C. Reynolds.** 2000. RgpA-Kgp peptide-based immunogens provide protection against *Porphyromonas gingivalis* challenge in a murine lesion model. Infect. Immun. **68:**4055–4063.
33. **Okamoto, K., T. Kadowaki, K. Nakayama, and K. Yamamoto.** 1996. Cloning and sequencing of the gene encoding a novel lysine-specific cysteine protease (Lys-gingipain) in *Porphyromonas gingivalis*: structural relationship with arginine-specific cysteine protease (Arg-gingipain). J. Biochem. **120:**398–406.
34. **Okamoto, K., K. Nakayama, T. Kadowaki, N. Abe, D. B. Ratnayake, and K. Yamamoto.** 1998. Involvement of a lysine-specific cysteine proteinase in hemoglobin adsorption and heme accumulation by *Porphyromonas gingivalis*. J. Biol. Chem. **273:**21225–21231.
35. **Percival, R. S., P. D. Marsh, D. A. Devine, M. Rangarajan, J. Aduse-Opoku, P. Shepherd, and M. A. Curtis.** 1999. Effect of temperature on growth, hemagglutination, and protease activity of *Porphyromonas gingivalis*. Infect. Immun. **67:**1917–1921.
36. **Pike, R., W. McGraw, J. Potempa, and J. Travis.** 1994. Lysine- and arginine-specific proteinases from *Porphyromonas gingivalis*. J. Biol. Chem. **269:**406–411.
37. **Pike, R. N., J. Potempa, W. McGraw, T. H. T. Coetzer, and J. Travis.** 1996. Characterization of the binding activities of proteinase-adhesin complexes from *Porphyromonas gingivalis*. J. Bacteriol. **178:**2876–2882.
38. **Potempa, J., R. Pike, and J. Travis.** 1995. The multiple forms of trypsin-like activity present in various strains of *Porphyromonas gingivalis* are due to the presence of either Arg-gingipain or Lys-gingipain. Infect. Immun. **63:**1176–1182.
39. **Potempa, J., J. Mikolajczyk-Pawlinska, D. Brassell, D. Nelson, I. B. Thogersen, J. J. Enghild, and J. Travis.** 1998. Comparative properties of two cysteine proteinases (gingipains R), the products of two related but individual genes of *Porphyromonas gingivalis*. J. Biol. Chem. **273:**21648–21657.
40. **Rangarajan, M., S. J. S. U. Smith, and M. A. Curtis.** 1997. Biochemical characterization of the arginine-specific proteases of *Porphyromonas gingivalis* W50 suggests a common precursor. Biochem. J. **323:**701–709.
41. **Revell, P. A., and V. L. Miller.** 2000. A chromosomally encoded regulator is required for expression of the *Yersinia enterocolitica inv* gene and for virulence. Mol. Microbiol. **35:**677–685.
42. **Sambrook, J., E. F. Fritsch, and T. Maniatis.** 1989. Molecular cloning: a laboratory manual, 2nd ed. Spring Harbor Laboratory Press, Cold Spring Harbor, N.Y.
43. **Shah, H., S. E. Gharbia, D. Kowlessur, E. Wilkie, and K. Brocklehurst.** 1990. Isolation and characterization of gingivain, a cysteine proteinase from *Porphyromonas gingivalis* strain W83. Biochem. Soc. Trans. **18:**578–579.
44. **Shi, Y., D. B. Ratnayake, K. Okamoto, N. Abe, K. Yamamoto, and K. Nakayama.** 1999. Genetic analyses of proteolysis, hemoglobin binding, and hemagglutination of *Porphyromonas gingivalis*: construction of mutants with a combination of *rgpA, rgpB, kgp*, and *hagA*. J. Biol. Chem. **274:**17955–17960.
45. **Slakeski, N., S. M. Cleal, and E. C. Reynolds.** 1996. Characterization of a *Porphyromonas gingivalis* gene *prtR* that encodes an arginine-specific thiol proteinase and multiple adhesins. Biochem. Biophys. Res. Commun. **224:**605–610.
46. **Slakeski, N., P. S. Bhogal, N. M. O'Brien-Simpson, and E. C. Reynolds.** 1998. Characterisation of a second cell-associated Arg-specific cysteine proteinase of *Porphyromonas gingivalis* and identification of an adhesin binding motif involved in association of the PrtR and PrtK proteinases and adhesins into large complexes. Microbiology **144:**1583–1592.
47. **Slakeski, N., S. M. Cleal, P. S. Bhogal, and E. C. Reynolds.** 1999. Characterization of a *Porphyromonas gingivalis* gene prtK that encodes a lysine-specific cysteine proteinase and three sequence-related adhesins. Oral Microbiol. Immunol. **14:**92–97.
48. **Slots, J.** 1982. Importance of black-pigmented *Bacteriodes* in human periodontal disease, p. 27–45. *In* R. J. Genco and S. Merganhagan (ed.), Host-parasite interaction in periodontal disease. American Society for Microbiology, Washington, D.C.
49. **Slots, J., L. Bragd, M. Wikström, and G. Dahlen.** 1986. The occurence of *Actinobacillus actinomycetemcomitans, Bacteroides gingivalis* and *Bacteroides intermedius* in destructive periodontal disease in adults. J. Clin. Periodontol. **13:**570–577.
50. **Tokuda, M., M. Duncan, M.-I. Cho, and H. K. Kuramitsu.** 1996. Role of *Porphyromonas gingivalis* protease activity in colonization of oral surfaces. Infect. Immun. **64:**4067–4073.
51. **Tokuda, M., T. Karunakaran, M. Duncan, N. Hamada, and H. Kuramitsu.** 1998. Role of Arg-gingipain A in virulence of *Porphyromonas gingivalis*. Infect. Immun. **66:**1159–1166.
52. **Tokuda, M., W. Chen, T. Karunakaran, and H. Kuramitsu.** 1998. Regulation of protease expression in *Porphyromonas gingivalis*. Infect. Immun. **66:**5232–5237.
53. **Travis, J., R. Pike, T. Imamura, and J. Potempa.** 1997. *Porphyromonas gingivalis* proteinases as virulence factors in the development of periodontitis. J. Periodont. Res. **32:**120–125.
54. **van Steenbergen, T. J., P. Kastelein, J. J. Touw, and J. de Graaff.** 1982. Virulence of black-pigmented *Bacteroides* strains from periodontal pockets and other sites in experimentally induced skin lesions in mice. J. Periodont. Res. **17:**41–49.
55. **Vicente, M. F., J. Mengaud, J. Chenevert, J. C. Perez-Diaz, C. Geoffroy, F. Baquero, P. Cossart, and P. Berche.** 1989. Reacquisition of virulence of haemolysin-negative *Listeria monocytogenes* mutants by complementation with a plasmid carrying the *hlyA* gene. Acta Microbiol. Hung. **36:**199–203.

Editor: R. N. Moore